charge transfer is of the order of a meter at the lower energies and at their target gas pressure of "about 10^{-4} Torr." They had an appreciably mixed beam at their observation point. If their pressure was 10^{-4} Torr, then nearly 30% of the beam would have been neutral at the 1 m point and at 10 keV.[15] (The beam at this distance would have been nearly 50% neutral at 2×10^{-4} Torr and at 10 keV.) It is difficult to fully assess the effects that collisions had on their results (see Sec. II).

†Supported by the National Science Foundation.
*NASA predoctoral trainee.

[1]R. H. Hughes, H. R. Dawson, B. M. Doughty, D. B. Kay, and C. A. Stigers, Phys. Rev. 146, 53 (1966).
[2]R. H. Hughes, H. R. Dawson, and B. M. Doughty, J. Opt. Soc. Am. 56, 830 (1966).
[3]R. H. Hughes, H. R. Dawson, and B. M. Doughty, Phys. Rev. 164, 166 (1967).
[4]D. R. Bates and J. C. G. Walker, Planetary Space Sci. 14, 1367 (1966).
[5]D. R. Bates and G. Griffing, Proc. Phys. Soc. (London) A66, 961 (1953).
[6]D. R. Bates and A. Dalgarno, Proc. Phys. Soc. (London) A66, 972 (1953).
[7]I. C. Percival and M. J. Seaton, Phil. Trans. Roy. Soc. London A251, 113 (1958).
[8]J. Van den Bos and F. J. de Heer, Physica 34, 358 (1967). Their expressions and tabulated values for the polarization are not correct. This conclusion is confirmed by R. K. L. L. Van den Eynde, FOM Institute for Atomic and Molecular Physics, Amsterdam, who has also obtained our Eq. (7) independently (private communication).
[9]R. H. Hughes, D. B. Kay, C. A. Stigers, and E. D. Stokes, Phys. Rev. 167, 26 (1968).
[10]H. E. Bethe and E. E. Salpeter, *Quantum Mechanics of One- and Two-Electron Systems* (Academic Press Inc., New York, 1957), p. 288.
[11]J. S. Murray, S. J. Young, and J. R. Sheridan, Phys. Rev. Letters 16, 439 (1966).
[12]J. L. Philpot and R. H. Hughes, Phys. Rev. 133, A107 (1964).
[13]J. L. Philpot, Ph.D. dissertation, University of Arkansas, 1965 (unpublished).
[14]J. G. Dodd, Ph.D. dissertation, University of Arkansas, 1965 (unpublished).
[15]Calculated by substituting the total stripping and charge-transfer cross sections tabulated by Allison [S. K. Allison, Rev. Mod. Phys. 30, 1137 (1958)] into Eq. (3).

Measured Shifts of Cesium Atomic Lines – Correlation with Electron Density Derived from Widths*

R. F. Majkowski and R. J. Donohue
Research Laboratories, General Motors Corporation, Warren, Michigan
(Received 12 April 1968)

The shifts of lines of the sharp, diffuse, and fundamental series of atomic cesium were measured for an rf electrodeless discharge in which the electron density was varied from 0.5 to 3×10^{14} cm^{-3} with a temperature range from 2600 to 3100°K. The shift values, which ranged from 0.008 to 1.4 Å, agree to ± 20% with the theoretical Stark-broadening predictions for the 6*P*-10*S*, 6*P*-11*S*, 6*P*-12*S* sharp-series members: 6*P*-9*D*, 6*P*-10*D*, 6*P*-11*D* diffuse-series members; and the 6*D*-5*F*, 6*D*-6*F*, 6*D*-7*F*, 6*D*-8*F* fundamental-series members. The measured shifts exhibit a definite trend with quantum number *n* for all three series. At low values of *n*, measured shifts are greater than those computed from Stark-broadening theory, whereas measured shifts are less than theory for high *n*. We show that certain assumptions in the Stark-broadening theory are not applicable to most of those lines where disagreement between theory and experiment is greatest.

INTRODUCTION

The profile of a spectral line is broadened, shifted, and made asymmetric by perturbations of the energy levels of the radiating atom. For a dense plasma (say from 10^{13} – 10^{17} electrons cm^{-3}), these perturbations are caused by the electric fields (Stark effect) in the vicinity of the radiating atom. Recent theories have predicted the width and shift as a function of the electron density and temperature of the plasma.[1] Calculations of the widths of neutral atom lines are the most reliable since they depend least on the approximations in the theory. For cesium, these widths have been accurately measured by several investigators,[2,3,4] and are within ± 10% of the predicted values. To test the completeness and self-consistency of the neutral line-profile theories, the complete spectral profile, i.e., the line shifts as well as shapes of cesium neutral-atom lines radiated from a plasma, were measured.

The shifts of four sharp (S) series lines, six diffuse (D) series lines, and five fundamental (F) series lines were measured at electron densities

from 0.5 to 3×10^{14} cm^{-3} with an electron temperature range from 2600 to 3100°K. These values are compared to the predicted values and the variance in these comparisons is accounted for in terms of the assumptions in the theoretical model.

LINE PROFILE CALCULATIONS

For the plasmas in these experiments, the principal mechanism which broadens spectral lines radiated by the plasma is Stark broadening. The most widely accepted Stark-broadening theory considers the electron contribution to the broadening in the impact approximation, and the ion broadening in the adiabatic and quasistatic approximation. If these approximations are applied to the profiles of atomic lines whose widths are much smaller than the separation of levels involved, the line profile[1,5] in reduced form is

$$J(x) = (1/\pi) W_\gamma(\beta) d\beta / [1 + (x - \alpha^{4/3}\beta^2)^2], \quad (1)$$

where $x = (\omega - \omega_0 - d)/w$, ω is the frequency, ω_0 is the frequency at peak intensity of the unperturbed line, d and w are the shift and half-width (at half-maximum intensity) due to electron impacts alone, β the reduced ion field, $W_\gamma(\beta)$ the reduced ion-field distribution, α the ion-broading parameter, $\alpha = (\alpha_i/w)^{3/4} N_e$, where α_i is the second-order Stark coefficient and N_e is the electron density.

The total (combined electron and ion) half-width and shift of this line profile are approximately[5]

$$w_t = [1 + 1.75\alpha(1 - 0.75R)]w, \quad (2)$$

$$d_t = [d/w + 2.0\alpha(1 - 0.75R)]w, \quad (3)$$

where R is the ratio of the mean ion separation to the Debye radius and is given by $R = 0.1 N_e^{1/6} T_e^{-1/2}$, and T_e is the electron temperature. The terms w and d are the half-widths and shifts due to electron impacts alone, and the second term is the ion-broadening contribution. The electron-impact terms w and d are directly proportional to N_e, and are only weak functions of T_e. The ion contribution is a much weaker function of the electron density since it depends on α, which is proportional to $N_e^{1/4}$, and R which is proportional to $N_e^{1/6}$. Equations (2) and (3) are valid when the ion contributions to the total line profile are small, i.e., for α below 0.5 and R less than 0.8. These requirements are fulfilled for all the plasma conditions and for all the lines for which measurements were made. The profiles may shift to either longer or shorter wavelengths depending on the details of the atomic energy-level structure. Thus the total width and total shift will be approximately proportional to the electron density.

EXPERIMENTAL ARRANGEMENT

Figure 1 schematically shows the over-all arrangement of the experimental apparatus. This system consists of: (1) two cesium plasma sources, (2) an optical imaging system, (3) a 3.4-m Ebert high-resolution spectrometer with a 300-groove/mm MIT grating, and (4) a quartz scanning monochromator.

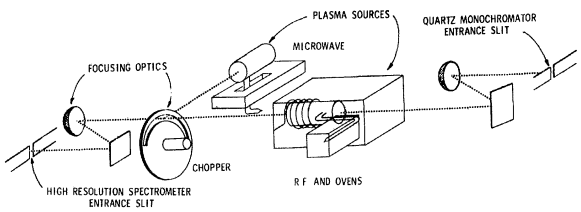

FIG. 1. Schematic view of over-all experimental arrangement.

Optical System

The principal measurements were the profiles of the spectral lines emitted by the radio-frequency-excited cesium plasma (rf plasma) source whose electron number density varied from approximately 0.5 to 3×10^{14} cm^{-3}. The feature that differentiates this arrangement from more conventional ones is the ability to measure the shift of a spectral line quickly and accurately. The very narrow lines emitted by the microwave-excited cesium plasma ($N_e \sim 10^{12} cm^{-3}$) give the fiduciary position (unshifted line) from which the shifts of the rf plasma line are measured. These two sources are focused sequentially onto the entrance slit of the high-resolution spectrometer. Light from the rf source is transmitted to the focusing optics through the slotted segment of a rotating chopper for a quarter of its rotation. During the next quarter cycle this light is cut off and the light from the microwave source is relfected from a mirrored segment of the chopper into the focusing system. This light chopper produces a photo multiplier signal which comes alternately from each light source and is displayed on a dual pen recorder synchronized with the optical chopper. An example of a line recording which has a "stepped" appearance due to the sequencing of both sources is shown in Fig. 2.

While the high-resolution spectrometer measures profiles of spectral lines from the rf plasma, a scanning monochromator and detector system (calibrated with a NBS tungsten-ribbon-filament standard lamp) measure the intensity of the continuum from the plasma. The continuum intensity was used to monitor the stability of the rf source during each run and to determine the electron temperature.

Plasma Sources

The rf cesium plasma is generated in an alkaline-resistant (Corning 1720) glass tube. This tube is a cylinder 10 cm long, 2.6 cm in diameter, with flat (Corning 1723) faces at either end. An arm protrudes from the tube and the cold spot of the tube is maintained at its tip. Hot dry air is fed into a quartz jacket surrounding the tube within an insulated box to control the main bulb temperature (Fig. 1). An electrodeless rf (8 Mc/

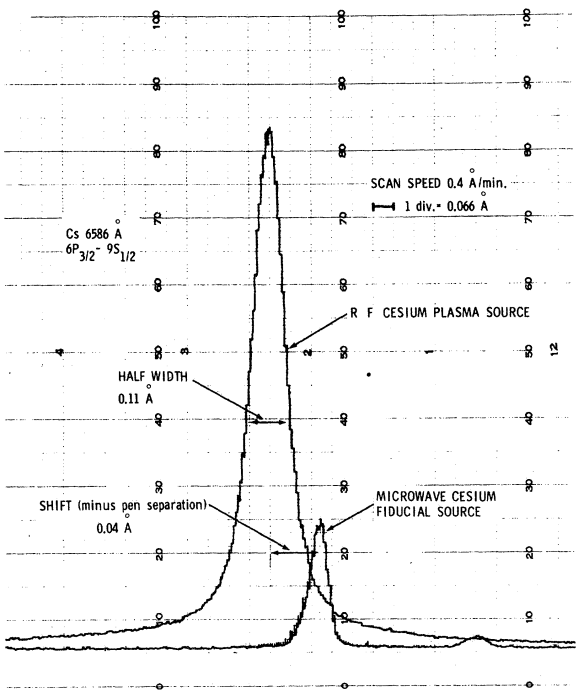

FIG. 2. Photomultiplier tracing for CsI 6586 Å. The rf plasma was at $N_e = 2.8\times10^{-14}$ cm^{-3} and the microwave plasma at $N_e = 10^{12}$ cm^{-3}. Rate of rotation of optical chopper was 54 rpm while the wavelength scan speed was 0.4 Å per minute.

sec) discharge is produced by a coil wrapped around the outer quartz jacket. It was possible to keep the electron density variations, measured by the continuum radiation, to ±10%.

A stable microwave-excited cesium discharge was the source of unperturbed cesium lines. The arm of a cesium-filled glass (1720) tube was positioned in the waveguide section of a 2.7-Gc/sec microwave generator (Fig. 1). A stable low-density plasma could be maintained at a coldspot (controlled by a small air jet) temperature of 100°C. The other parts of the tube were heated by a heater tape to 180°C. The measured half-widths of the spectral lines from this source were equal to the instrument half-width, 0.04 Å at 5500 Å.

WIDTH AND SHIFT MEASUREMENTS

The profiles of eight S-series lines, ten D-series lines, and nine F-series lines were recorded at a minimum of five different plasma conditions. The electron density was derived from the line widths by Eq. (2) and Griem's values[5] of w, R, and α (iterating once to account for the small variation of α and R with N_e). The electron density (Table I) was an average taken over at least ten lines which were optically thin (free from absorption) with a deviation from the mean of ±10%. The electron temperature (Table I) was measured from the relative intensity of the free-bound continuum

TABLE I. Experimental plasma conditions.

Electron number density (N_e) (10^{-14} cm^{-3})	Electron temperature (T_e) (°K)
0.48	2800
0.7	3100
0.9	2800
1.0	2630
1.1	2630
2.8	2900

to the $6P$ doublet using the empirical equation developed by Agnew[3] based on Mohler's[6] experiments.

Figures 3, 4, 5 show the spectral line shifts versus electron density N_e (determined from the measured spectral width) for the S, D, and F series lines. The solid line represents the theoretical line shift d_t (computed from Eq. 3) for a given principal quantum number n. The sets of data points are the measured line shifts d_m for a given n. The dotted line following a least-squares fit of the data has been drawn for each value of n. These dotted lines represent the average measured shift values as a function of electron density for a given principal quantum number. The measured curves are approximately parallel to the theoretical curves and their slopes are about 45° on the log-log plot.

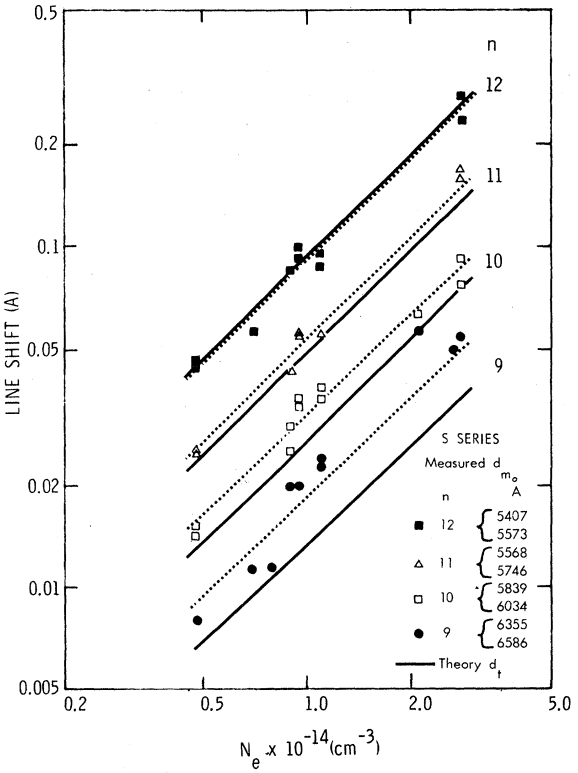

FIG. 3. Measured shift (d_m) and theoretical shift (d_t) versus N_e for S-series lines. Average of the doublets $6P_{1/2} - nS_{1/2}$ and $6P_{3/2} - nS_{1/2}$.

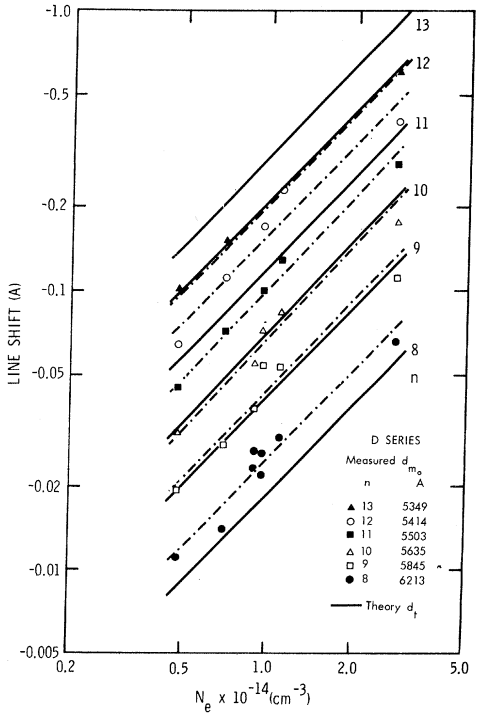

FIG. 4. Measured shift (d_m) and theoretical shift (d_t) versus N_e for D-series lines $6P_{3/2} - nD_{5/2}$. Negative line shift corresponds to a decrease in wavelength.

This slope indicates the same linear relationship between N_e and d_m as for N_e and d_t. The theoretical shifts of the sharp-series lines are the average of the shift of the doublets $6P_{1/2}$-$nS_{1/2}$ and $6P_{1/2}$-$nS_{1/2}$ for $n = 9$, 10, 11, and 12. The sharp-series data points in Fig. 3 include both members of the series at most of the N_e values (of Table I) with single lines at additional N_e values.

The D-series shift values in Fig. 4 are for the $6P_{3/2}$-$nD_{5/2}$ lines at $n = 8$, 9, 10, 11, 12, and 13. The shifts of another branch of the $6P$-nD series, viz. $6P_{1/2} - nD_{3/2}$, were measured and their variation with N_e was similar to that in Fig. 4. The $6P_{3/2} - nD_{3/2}$ lines were not measured since the intensity of these lines is much weaker than the other members of the diffuse series. The data for both branches of the $5D - nF$ series, $5D_{5/2} - nF_{5/2, 7/2}$ and $5D_{3/2} - nF_{5/2}$ are plotted in Fig. 5 for $n = 5$, 6, 7, 8 at most N_e values (of Table I) with single lines at additional N_e values. The $5D_{5/2} - 9F_{5/2, 7/2}$ line is the only member of the $9F$ branch measured. The predicted shifts of both branches are almost identical; therefore a single theoretical curve is plotted for each n value.

The $6P - nS$ and the $5D - nF$ series lines shift to longer wavelengths, and the $6P - nD$ series lines shift to shorter wavelengths, as predicted. These data were taken at electron temperatures from 2630 to 3100°K so that some degree of scatter is expected, although scatter due to this temperature variation should not exceed ± 10%. For this reason no attempt was made to reduce the data to a common temperature.

The data of Figs. 3, 4, and 5 are summarized in Fig. 6 where the average ratio of d_m/d_t for the entire range of N_e is plotted for a given n for each of the three spectral series. The flags on the average d_m/d_t values are the rms deviations of the data points. The curves of Fig. 6 show the general agreement of the spectral measurements with theory over this range of plasma conditions. Only the average value for $n = 9$ of the F series, $n = 8$, 12, and 13 of the D series, and $n = 9$ of the S series are outside an arbitrary agreement level of ± 20%.[7] From this group, the variation flags of the average values for $n = 9$ and 12 of the D series and the $n = 9$ of the S series do fall within these limits. The negative slope of all three curves is perhaps more interesting than the disagreement of some of the predicted shifts with the data. Some disagreement can be expected in view of the inherent approximations in the theory.

LINE PROFILES

The measured profiles of S-, D-, and F-series lines were compared with the theoretical profiles of Eq. (1). The profiles differ in the

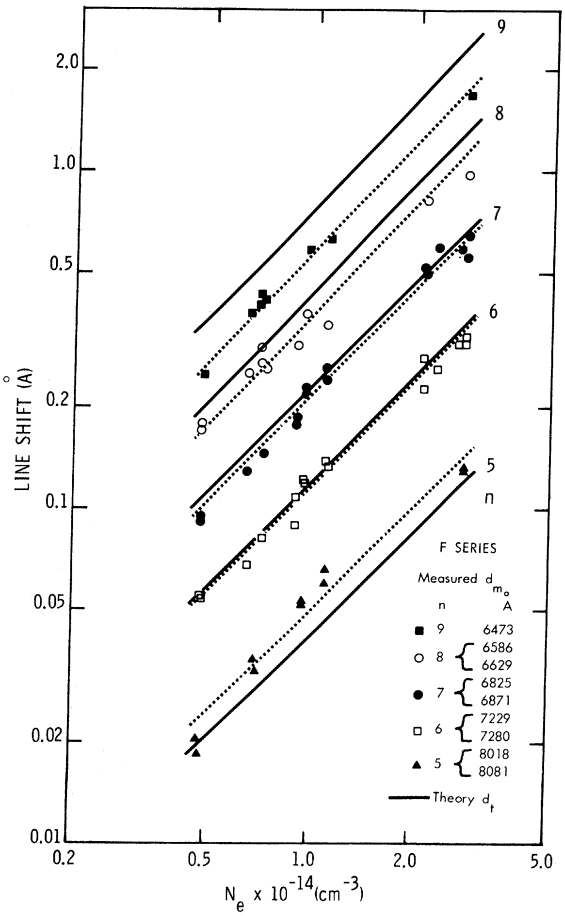

FIG. 5. Measured shift (d_m) and theoretical shift (d_t) versus N_e for F-series lines $5D_{5/2} - nF_{5/2, 7/2}$.

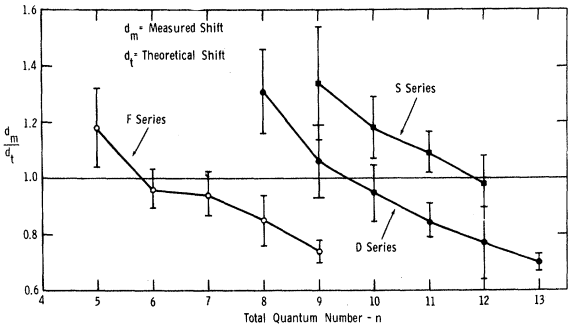

FIG. 6. Ratio of measured–to-theoretical shift versus total quantum number for the F, D, and S series.

position of the line peak (shift) and in the asymmetry of the wings of the lines. This difference is small for S lines and lower members of the D series. The difference increases for higher members of the D series and most of the F series lines. A representative display of the difference occurs in the profile of the $5D_{3/2} - 7F_{5/2}$ line shown in Fig. 7.

A comparison of the asymmetry of the wings computed from the asymptotic equation for the profile yields a value for the parameter α of 0.15 where the theoretical value is 0.22. This reduction in α is consistent with a measured shift smaller than the theoretical shift value.

ERROR ANALYSIS

The accuracy with which the Stark-width-broadening theory of Griem predicts the electron density at 9×10^{13} cm^{-3} in a cesium plasma (for the widths of the optically thin lines which we use) has been ascertained to be ±10%.[4] This uncertainty combined with our reproducibility of these line shapes of ± 5% gives a maximum uncertainty of ±15% in the determination of N_e. The shift measurements are reproducible to ± 0.005 Å. This limitation is caused by the uncertainty in the position of the peak of the line combined with the variation of the recorder-pen displacement. To attribute the large d_m values (compared with theory) for the low S - series members to this uncertainty, we believe, is precluded by the data of the 9 and 10 S - series lines. The peaks of these lines were the sharpest and most accurately determined. Yet the constant displacement between measurement and theory

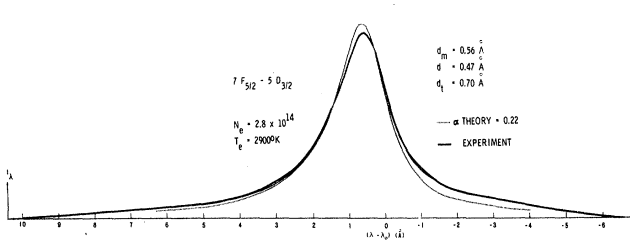

FIG. 7. Experimental and theoretical line profiles for $7F_{5/2} - 5D_{3/2}$.

extends over the range of shift values from 0.008 to 0.1 Å.

The electron-temperature measurement from the continuum slope appears to be accurate to ± 10% and is probably more like ± 5%. The width and shift values are insensitive to this temperature which therefore does not influence the accuracy quoted above for this shift measurement.

An experimental error of 0.005 Å in shift would correspond to an uncertainty in N_e of ± 2% at an N_e of 10^{14} cm^{-3} for the $9F$ lines, ± 15% for the $9D$ lines, and ± 45% for the $9S$ lines from the theoretical curves in Figs. 3, 4, and 5. Since meaningful width measurements require optically thin lines, we measured only broad lines for which the quoted uncertainty in N_e (from width data) is ± 10%. Accuracy of this magnitude may be obtained in the shifts of lines entirely unsuitable for width measurements but highly desirable for other reasons. An example is the relatively large shift of the $10S$, $11S$, and $12S$ members of the sharp series which have high intensity but small widths.

Furthermore, self-absorption and broadening of the spectral lines tend to be symmetric, so that the shift is not affected by these phenomena. This fact is evidenced by the reasonable correlation of the shift measurements with theory between the $6P$-$8D$, $6P$-$9D$, and $5D$-$5F$ lines whose widths, because of absorption effects, yielded N_e values between three and ten times the values obtained from optically thin lines. This allows density measurements in plasmas where only the low-series members may have sufficient intensity but may also be absorption-broadened and therefore preclude a width measurement.

Also, the shift measurement lends itself to photographic techniques, where a standard spectrum can be superimposed on the cesium spectrum, and where an intensity calibration of the photographic emulsion is not necessary.

VALIDITY OF THEORETICAL APPROXIMATIONS

The differences between theoretical predictions and experimental data as shown in Fig. 6 for certain lines might be expected because of a breakdown of one or more of the approximations inherent in the Stark-broadening theory. There are three major assumptions in the theory; (1) the classical path treatment of the electrons, (2) the neglect of Debye shielding in the impact theory, and (3) the isolation of the upper states.

The first two assumptions affect the electron-impact shift and the third assumption affects the ion contribution to the shift and line-profile asymmetry. The criteria for the validity of these approximations are:

Classical Path $kT_e >> w_{\alpha\alpha'}$,
Isolated Line $w_{\alpha\alpha'} >> w_t$,
Debye Shielding $w_{\alpha\alpha'} >> w_p$,

where $w_{\alpha\alpha'}$ is the separation of the upper state from the nearest interacting level, w_t is the half-width of the line profile, and w_p is the plasma frequency.

All of these approximations deal with the manner

in which the interaction between radiators and perturbers are treated or with how the mutual interaction of perturbers are introduced into the theory. Consequently, the most critical test of these approximations would occur at the highest density of perturbers. The possible breakdown of these assumptions at the highest electron density might also explain the discrepancies with theory observed in Fig. 6. In order to evaluate this possibility, Table II lists w_p, kT_e, $w_{\alpha\alpha'}$, and w_t for all the lines measured at the highest electron density (2.8×10^{14} cm^{-3}) along with the average value of d_m/d_t.

In the F series, the 8 and 9 levels do not fulfill the criteria for either the isolated line or Debye shielding approximations. At increasing quantum numbers, the breakdown of the isolated-line approximation leads to smaller d_m/d_t ratios because of an expected change of the Stark coefficient from the quadratic term (finite shift) to the linear term (zero shift).

A similar effect is observed for the higher-quantum-number levels in the D series. The 13D level does not fulfill the isolated-line and Debye-shielding conditions, whereas for the 12D line the isolated-line criterion is marginally fulfilled. Therefore we would expect that d_m/d_t for the 12D would fall within our 20% agreement limit, but it does not. For similar validity-criteria ratios in the 7F line, we see good agreement in the d_m/d_t ratio (0.94). Thus it appears that the Debye-shielding criterion is not as critical for the F series as for the D series.

A more significant observation in the diffuse series is that, while the 8D level fulfills all the stated approximations, the measured average-shift value does not fall within our validity limits. It is this measurement as well as that of the 5F line that in large part establishes the negative slopes observed in Fig. 6. It would be instructive to determine whether this trend of increasing d_m/d_t with decreasing quantum number continues at lower n values. No additional transitions exist below $n=5$ in the visible or near-infrared spectral regions for the 5D-nF series. But transitions with $n=6$ and 7 in the 6P-nD do exist in this spectral region. Shift measurements of these lines could confirm the observed trend of d_m/d_t versus n.

The 6P-9S line of the sharp series does not meet the classical-path approximation, whereas the 10S line may only marginally conform to it. In the S series, as the lines fall within the classical-path approximation, the d_m/d_t ratio also falls within the agreement limits.

TABLE II. Frequency separation $w_{\alpha\alpha'}$ to nearest interacting level, total measured linewidth w_t, and measured-to-theoretical shift ratio at $N_e = 2.8 \times 10^{14}$ cm^{-3}, $w_p = 5$ cm^{-1}, $kT_e = 1750$ cm^{-1}.

Levels	$w_{\alpha\alpha'}$ (cm^{-1})	w_t (cm^{-1})	d_m/d_t
5D-5F	38	0.3	1.18
5D-6F	18	1.0	0.96
5D-7F	10	2.1	0.94
5D-8F	6	4.6	0.85
5D-9F	4	6.2	0.74
6P- 8D	141	0.3	1.32
6P- 9D	82	0.6	1.06
6P-10D	52	1.2	0.95
6P-11D	35	2.0	0.85
6P-12D	25	3.8	0.77
6P-13D	18	7.0	0.70
6P- 9S	724	0.07	1.34
6P-10S	427	0.16	1.18
6P-11S	273	0.34	1.09
6P-12S	186	0.70	0.99

CONCLUSIONS

Electron density in a cesium plasma can be determined from measured line shifts to an accuracy of ±30% for the lines measured in this paper for electron densities of 10^{13} to 10^{15} electrons/cm^3. This conclusion assumes that electron densities as measured by line width are accurate to within ±10%.[3,4]

The observed line shifts differ from theoretical line shifts in a systematic way. The ratio of observed-to-theoretical shifts decreases as the total quantum number increases. For small values of total quantum number, this ratio is greater than unity, and for large values, less than unity. The agreement of observed with theoretical line shifts is best where the approximations of the theory are strictly satisfied.

ACKNOWLEDGMENTS

The authors are indebted to H. R. Griem of the University of Maryland for his suggestions concerning the analysis of the profile data. We thank F. E. Jamerson for his encouragement and support of this project, and John Price for his technical assistance.

*This study was supported in part by National Aeronautics and Space Administration.

[1]H. Griem, M. Baranger, A. C. Kolb, and G. Oertel, Phys. Rev. 125, 177 (1962); H. Griem, Phys. Rev. 128, 515 (1962).

[2]R. Donohue and R. Majkowski, J. Appl. Phys. 33, 3, (1962); W. Reichelt and W. Kruer, Thermionic Conversion Specialist Conference, San Diego, California, 1965, Los Alamos Report No. LA-DC-7390.

[3]P. Stone and L. Agnew, Phys. Rev. 127, 1157 (1962).

[4]S. Gridneva and G. Kasalov, in Proceedings of the Seventh International Conference on Phenomena in Ionized Gases, Belgrade, 1965, edited by B. Perovic and D. Fosic (Gradevinska Knjiga Publishing House, Belgrade, 1966).

[5]H. Griem, Plasma Spectroscopy (McGraw-Hill Book Co., Inc. New York, 1965).

[6]F. Mohler, J. Res. Natl. Bur. Standards 17, 849 (1937), F. Mohler, Rev. Mod. Phys. 1, 216 (1929).

[7]The ± 20% agreement level for these shift measurements is reasonable when compared to the maximum uncertainty of ±15 in width measurements (see the "Error Analysis" section).

Polarization Potential in Low-Energy Electron-H_2 Scattering*

Neal F. Lane†
Rice University, Houston, Texas
and
Ronald J. W. Henry
Kitt Peak National Observatory,‡ Tucson, Arizona
(Received 21 March 1968)

An adiabatic polarization potential appropriate to low-energy electron-H_2 scattering has been calculated by a variational approach. The total energy of the static electron-H_2 system is minimized with respect to the parameters $C_{\alpha\beta}$ in a trial function of the form

$$\psi_0(1,2)\sum_{\alpha,\beta} C_{\alpha\beta}(x_1+x_2)^{\alpha}(z_1+z_2)^{\beta},$$

where $\psi_0(1,2)$ is Joy and Parr's one-center ground-state function. The subscripts 1 and 2 refer to the molecular electrons. The polarization potential is found to be well represented by $v_p^0(r)+v_p^2(r)P_2(\cos\theta)$, where θ specifies the position vector of the static electron with respect to the internuclear axis. The radial functions $v_p^0(r)$ and $v_p^2(r)$ have been determined over a wide range in r. The polarization potentials are used in a calculation of rotational-excitation cross sections. Comparisons are made with results of other investigations.

I. INTRODUCTION

In electron-atom scattering, distortion of the target atom by the incident electron is very important. For sufficiently large electron energies, this distortion process is highly nonadiabatic and results in excitation of the target atom. In the case of electron energies below the threshold for excitation, the atom may be thought of as being "polarized" by the electron, which then moves in a potential field modified by the effects of this polarization. When the velocity of the incident electron is small, compared to that of the bound atomic electrons; the adiabatic approximation may be invoked. It is then appropriate to define an adiabatic polarization potential $V_P(r)$ which has the asymptotic behavior

$$V_P(r)_{r\tilde{\to}\infty} - \alpha/2r^4, \tag{1}$$

where α is the electric polarizability of the atom. The simplest method for approximating the effects of polarization is to construct some analytic form for the potential[1-3] which has asymptotic behavior (1). Often, the potential is adjusted so as to yield cross sections consistent with experiment. However, such an approach is not very satisfactory. A better technique for the treatment of polarization effects in electron-atom collisions, is Temkin's method of polarized orbitals.[4] This method, which employs first-order perturbation theory to obtain the atomic orbitals in the field of the scattered electron, has been successfully used for various atomic systems.[4-10]

In electron collisions with diatomic molecules, much of what we have said still holds true. Because of the non-spherical character of diatomic molecules, however, the polarizability is not spherically symmetric. Thus the asymptotic form for the adiabatic polarization potential becomes [11]

$$V_P(\vec{r})_{r\tilde{\to}\infty} - \alpha_0/2r^4 - (\alpha_2/2r^4)\,P_2(\hat{r}\cdot\hat{R}), \tag{2}$$

where $\alpha_0 = (\alpha_z + 2\alpha_x)/3$,

and $\alpha_2 = 2(\alpha_z - \alpha_x)/3$.

Here α_z and α_x are the respective polarizabilities (in units of a_0^3), parallel and perpendicular to the internuclear axis $\hat{R}$. Polarization effects in electron-molecule collisions are particularly interesting, since rotational and even vibrational excitation of the molecule is possible at relatively low energies, where the adiabatic approximation might still be expected to be good. Thus, we can investigate, within the adiabatic framework, the effects of polarization on inelastic scattering. As in the case of atoms, it has previously been the practice to construct an analytic polarization potential with asymptotic form (2). The parameters of this potential can be adjusted so that calculated elastic cross sections agree with either low-energy momentum-transfer measurements,[12] or total cross sections observed at higher energies.[13] However, since all partial waves are not affected by the potential in the same way, comparison with the low-energy measurements can be misleading. For example, p-wave scattering, which is dominant for rotational excitation, may not be given correctly, since the momentum-transfer cross section at low energies is primarily due to s-wave scattering. When the potential is adjusted to fit